Article

Cell

DNA-Demethylating Agents Target Colorectal Cancer Cells by Inducing Viral Mimicry by Endogenous Transcripts

Graphical Abstract

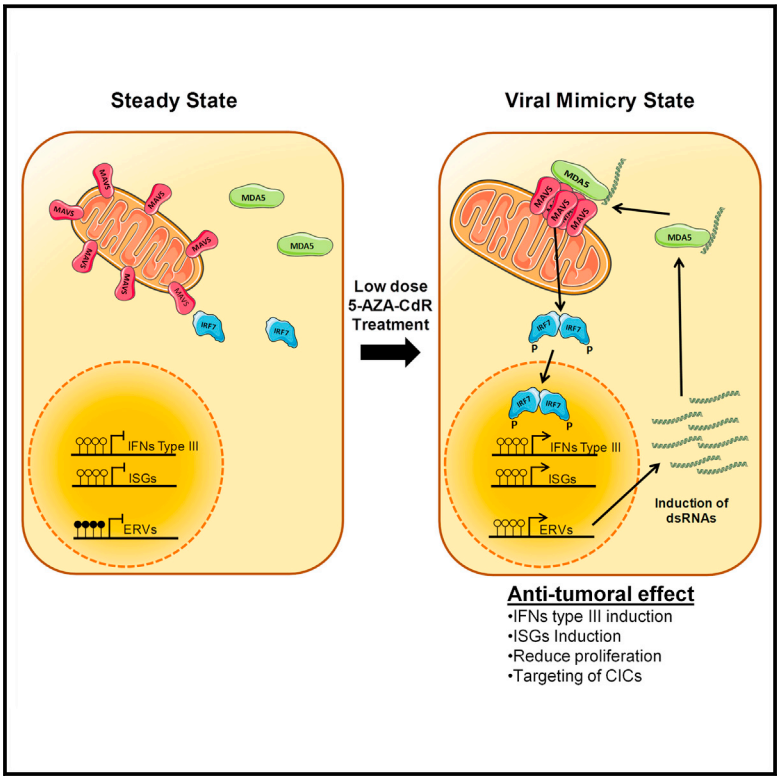

Authors

David Roulois, Helen Loo Yau, Rajat Singhania, ..., Trevor J. Pugh, Catherine O'Brien, Daniel D. De Carvalho

Correspondence

ddecarv@uhnres.utoronto.ca

In Brief

Anti-tumor DNA-demethylating agents act by inducing transcription of endogenous dsRNAs that activate the viral recognition and interferon response pathway. This anti-viral response reduces proliferation of colorectal cancer-initiating cells.

Highlights

- 5-AZA-CdR induces formation of dsRNAs and activation of the MDA5/MAVS/IRF7 pathway
- An anti-proliferative response to DNA demethylation is mediated by viral mimicry
- 5-AZA-CdR-mediated targeting of CICs is mainly mediated by viral mimicry
- The MDA5/MAVS/IRF7 pathway is a potentially druggable target against colorectal cancer

Accession Numbers

GSE62086

Roulois et al., 2015, Cell *162*, 961–973
August 27, 2015
http://dx.doi.org/10.1016/j.cell.2015.07.056

CellPress

Cell

DNA-Demethylating Agents Target Colorectal Cancer Cells by Inducing Viral Mimicry by Endogenous Transcripts

David Roulois,[1] Helen Loo Yau,[1,2] Rajat Singhania,[1] Yadong Wang,[1] Arnavaz Danesh,[1] Shu Yi Shen,[1] Han Han,[4] Gangning Liang,[4] Peter A. Jones,[4,6] Trevor J. Pugh,[1,2] Catherine O'Brien,[1,3,5] and Daniel D. De Carvalho[1,2,*]
[1]Princess Margaret Cancer Centre, University Health Network, Toronto, ON M5G 2M9, Canada
[2]Department of Medical Biophysics, University of Toronto, Toronto, ON M5G 2M9, Canada
[3]Department of Laboratory Medicine and Pathobiology, University of Toronto, Toronto, ON M5S 1A1, Canada
[4]Department of Urology, Keck School of Medicine, University of Southern California, Los Angeles, CA 90089, USA
[5]Department of Surgery, Toronto General Hospital, Toronto, ON M5T 1P5, Canada
[6]Present address: Van Andel Research Institute, Grand Rapids, MI 49503, USA
*Correspondence: ddecarv@uhnres.utoronto.ca
http://dx.doi.org/10.1016/j.cell.2015.07.056

SUMMARY

DNA-demethylating agents have shown clinical anti-tumor efficacy via an unknown mechanism of action. Using a combination of experimental and bioinformatics analyses in colorectal cancer cells, we demonstrate that low-dose 5-AZA-CdR targets colorectal cancer-initiating cells (CICs) by inducing viral mimicry. This is associated with induction of dsRNAs derived at least in part from endogenous retroviral elements, activation of the MDA5/MAVS RNA recognition pathway, and downstream activation of IRF7. Indeed, disruption of virus recognition pathways, by individually knocking down MDA5, MAVS, or IRF7, inhibits the ability of 5-AZA-CdR to target colorectal CICs and significantly decreases 5-AZA-CdR long-term growth effects. Moreover, transfection of dsRNA into CICs can mimic the effects of 5-AZA-CdR. Together, our results represent a major shift in understanding the anti-tumor mechanisms of DNA-demethylating agents and highlight the MDA5/MAVS/IRF7 pathway as a potentially druggable target against CICs.

INTRODUCTION

Many tumor types are organized as a cellular hierarchy sustained by a subpopulation of cancer-initiating cells (CICs) (Kreso and Dick, 2014). These CICs possess unique features, including long-term self-renewal, the ability to initiate tumor growth in xenograft models, and the ability to differentiate into the bulk of the tumor mass (Kreso and Dick, 2014). Colorectal cancer follows this hierarchical model and contains CICs (Dalerba et al., 2007; O'Brien et al., 2007, 2012; Ricci-Vitiani et al., 2007). Colorectal CICs are believed to play a major role in tumor relapse and patient survival, suggesting that therapeutic strategies targeting this cell population would be highly beneficial to patient outcome (Kreso et al., 2014; Merlos-Suárez et al., 2011).

Recent work suggests that CICs can be targeted by epigenetic therapies, including experimental BMI-1 inhibitors in colorectal cancers and FDA-approved DNA methylation inhibitors, such as 5-aza-2-deoxycytidine (5-AZA-CdR) in hematological malignancies (Kreso et al., 2014; Tsai et al., 2012). 5-AZA-CdR is a cytidine analog that traps DNA methyltransferases after incorporation into DNA, resulting in proteasomal degradation and global DNA demethylation (Kelly et al., 2010).

There is an ongoing debate about the molecular mechanisms underlying the clinical efficacy of 5-AZA-CdR and whether it represents a direct consequence of its effect on global demethylation (Issa and Kantarjian, 2009). Previous data suggest that promoter demethylation, followed by gene re-activation of aberrantly methylated tumor suppressor genes (TSGs), is a major mechanism of 5-AZA-CdR anti-tumor effects (Navada et al., 2014). This is in line with the finding that many TSG promoters are hypermethylated in cancer cells and that cancer cells become epigenetically addicted to DNA hypermethylation of a set of TSGs (De Carvalho et al., 2012). More recently, we demonstrated that gene-body DNA demethylation, followed by gene repression of oncogenic pathways, may also play a role in the cancer response to 5-AZA-CdR (Yang et al., 2014). However, the prolonged time to response observed in patients and the fact that global DNA methylation profiling, neither pretreatment nor during treatment, can predict response (Treppendahl et al., 2014) suggests that the major molecular mechanisms underlying the clinical efficacy of 5-AZA-CdR may lie beyond demethylation of TSG promoters and oncogene gene-bodies.

Here, we describe that transient low-dose exposure to 5-AZA-CdR targets colorectal CICs by inducing double-stranded RNA (dsRNA) expression, activation of the cytosolic pattern recognition receptor MDA5, and downstream activation of MAVS and IRF7. This will lead to a "viral mimicry" state and is a major molecular mechanism for the anti-tumor effect mediated by a transient low dose of 5-AZA-CdR.

RESULTS

Transient Low-Dose 5-AZA-CdR Induces Four Different Profiles of Gene Expression

We have recently shown that transient treatment of HCT116 colorectal cancer cells with a low dose (0.3 μM) of 5-AZA-CdR

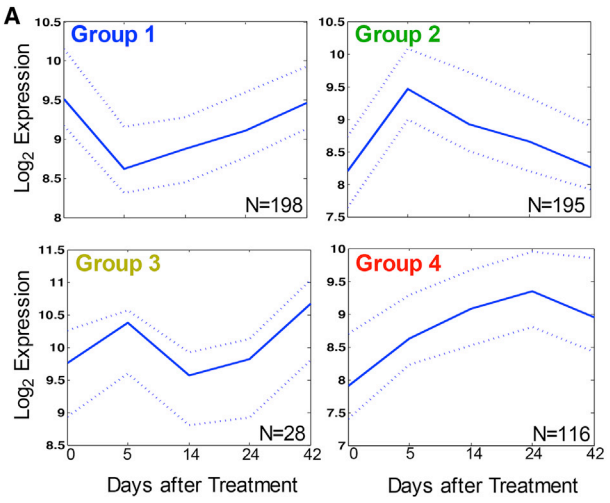

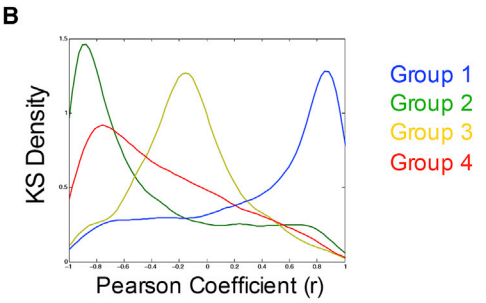

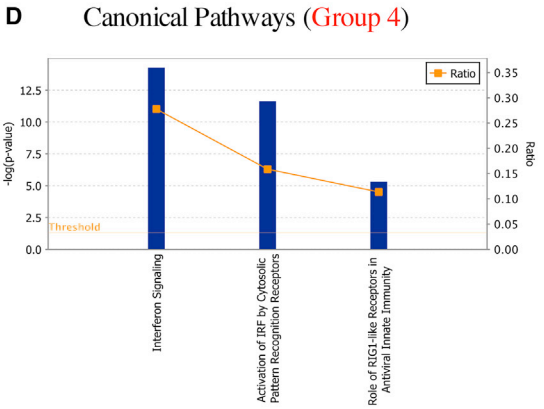

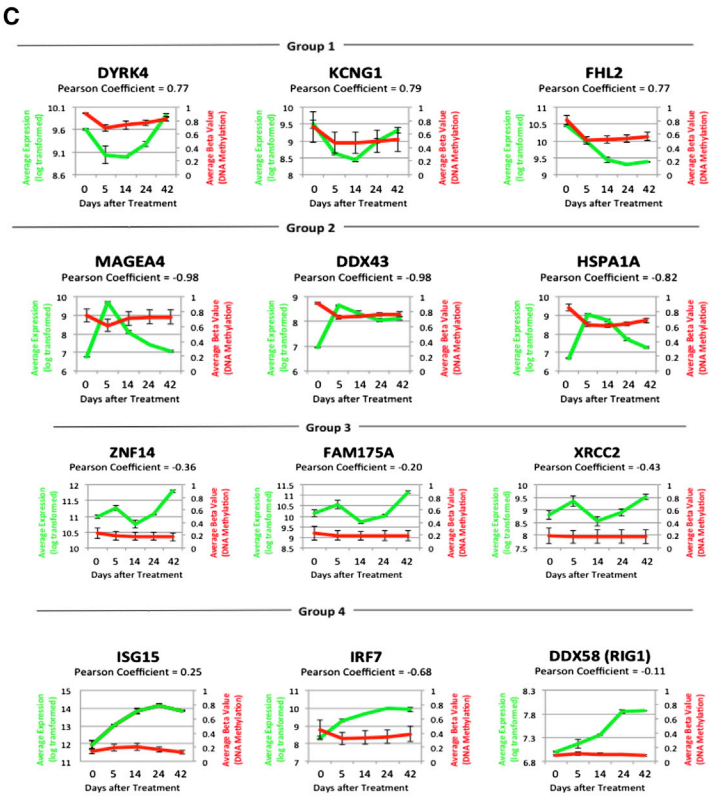

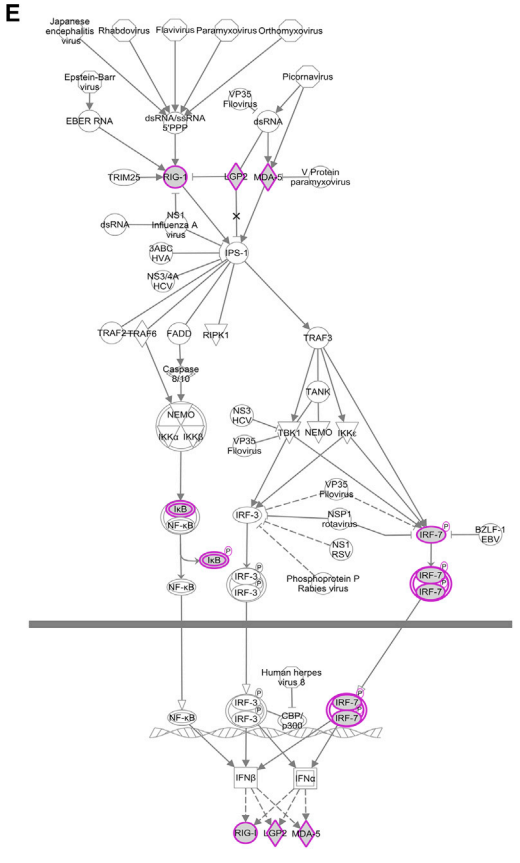

(legend on next page)

for 24 hr, followed by cell culture in a drug-free medium has a long-term effect on population doubling time and colony-formation ability (Yang et al., 2014). Here, we used the same experimental system to test the effects of transient treatment of 5-AZA-CdR on gene expression patterns. We monitored gene expression patterns before and after treatment for up to 42 days after drug withdrawal. Using gene expression microarray and consensus clustering to classify the most variable genes, we identified four patterns of gene expression (Figures 1A and S1A–S1C). Groups 1 and 2 are early-response genes that are either downregulated (group 1) or upregulated (group 2) within 5 days of 5-AZA-CdR treatment, but return to the original expression level by the end of the follow-up period (42 days) (Figure 1A). Using DNA methylation BeadChips, we observed that group 1 genes have a strong positive correlation between expression and DNA methylation (Figures 1B and 1C), with most of the DNA methylation changes occurring at gene bodies. Group 2 genes have a strong negative correlation between expression and DNA methylation (Figures 1B and 1C). Group 3 is a small and noisy group presenting no correlation between expression and DNA methylation (Figures 1A–1C). Group 4 genes are late-response genes, where peak gene expression occurs 24 days after initial exposure to 5-AZA-CdR and higher gene expression levels are observed even up to 42 days after drug withdrawal (Figure 1A). This delayed activation and sustained gene expression is compelling, since most clinical responses to 5-AZA-CdR are delayed (Treppendahl et al., 2014). Group 4 genes have a weaker anti-correlation between expression and DNA methylation, with a fat tail around the weak and no correlation region (correlation coefficient, r; between −0.5 and +0.5; Figures 1B and 1C), suggesting that several genes in this group are activated by 5-AZA-CdR in the absence of direct changes in DNA methylation of their promoters or coding regions. Most of the genes in this group have low DNA methylation levels pretreatment (Figure 1C), suggesting that their activation by drug treatment does not involve promoter DNA demethylation.

Late-Response Genes Are Enriched for Interferon-Responsive Genes and the RIG1/MDA5 RNA-Sensing Pathway

To identify the most significant canonical pathways associated with the late-response genes (group 4), we performed an ingenuity pathway analysis. Using Fisher's right-tailed exact test, we identified "interferon signaling" (p value = 5.35^{-15}; Figure S1D), "activation of IRF by cytosolic pattern recognition receptors" (p value = 2.37^{-12}; Figure S4), and "role of RIG-1-like receptors in antiviral innate immunity" (p value = 5^{-06}, Figure 1E) as the top three enriched canonical pathways at the ingenuity knowledge database (Figure 1D). Interestingly, recent work reporting activation of interferon-responsive genes and the RIG1/MDA5 pathway after patient treatment with DNA methylation inhibitors at low doses (Wrangle et al., 2013) highlights the clinical relevance of our model system.

Although most of the genes in group 4 are responsive to type I interferon (IFN) (Figures 1D and S1D), we could not detect any IFNα or IFNβ transcripts or protein as measured by qPCR and ELISA in HCT116, LIM1215, and HT29 colorectal cancer cells before or after a transient low dose of 5-AZA-CdR treatment. Thus, this suggests that the cytosolic pattern recognition receptors RIG1/MDA5 may be initiating the signaling cascade rather than type I interferon. To test this hypothesis, we took advantage of the fact that the RIG1/MDA5 signaling cascade depends on the adaptor molecule MAVS (mitochondrial antiviral signaling, also known as IPS1, CARDIF, and VISA) (Barbalat et al., 2011). MAVS is an essential adaptor molecule that connects RIG1 and MDA5 activation to the downstream activation of IRF3 and IRF7 (Figure 1E). Previous work has established that MAVS knockdown blocks the RIG1/MDA5 signaling pathway (Barbalat et al., 2011), allowing us to test the effect of low-dose 5-AZA-CdR treatment when the RIG1/MDA5 signaling pathway is impaired.

First, we treated the B16-blueTM IFN-α/β Cells (InvivoGen) with 5-AZA-CdR for 24 hours. B16-blue cells are stably transfected with a SEAP (Secreted embryonic alkaline phosphatase) reporter gene under the control of *isg54* promoter enhanced by a multimeric ISRE (interferon-sensitive response element) and will respond to the activation of STAT1, STAT3, IRF3, IRF7, and IRF9. Therefore, B16-blue cells can detect bioactive type I IFNs by monitoring the activation of STAT1/2 (Figure S1D); in addition, they can detect activation of the RIG1/MDA5 pathway by monitoring activation of IRF3/7 (Figure 1E).

We observed that upon transient low-dose 5-AZA-CdR exposure, B16-blue cells initiate the strong activation of the SEAP reporter gene (Figure 2A). This 5-AZA-CdR-mediated activation of the SEAP reporter gene was blocked by MAVS knockdown (Figures 2A, S2A, and S2B). These data highlight the importance of RIG1/MDA5 cytosolic receptors in inducing the activities of interferon-responsive promoters in response to 5-AZA-CdR treatment. To test this further, we incubated untreated B16-blue cells

Figure 1. Transient Low-Dose Treatment of 5-AZA-CdR Induces Durable and DNA Demethylation-Independent Activation of a Gene Set Enriched for Interferon-Responsive Genes and the RIG-1 Pathway

(A–E) HCT116 cells were transiently treated with 0.3 μM of 5-AZA-CdR for 24 hr (one population doubling time). RNA was extracted before treatment and at day 5, 14, 24, and 42 after drug withdrawal and subjected to cDNA microarray. (A) An expression profile for each of the four identified clusters. The solid line represents the median value for each group, and the dotted lines are the lower quartile (lower dotted line) and the upper quartile (upper dotted line) for each group. (B) Kernel density plots showing the Pearson correlation (r) between gene expression and DNA methylation for each probe across the 42-day time course experiment. The y axis indicates the density of probes. (C) Selected examples of genes from groups 1, 2, 3, and 4 are shown. Left: the y axis represents the average expression level. The y axis represents the average expression level (left) and the average DNA methylation level (right). The x axis denotes time (in days) after 5-AZA-CdR withdrawal. Error bars represent the SD. (D) The three most significant canonical pathways enriched at group 4 genes using ingenuity pathway analysis. The significance value for each canonical pathway was calculated by Fisher's exact test right-tailed. The y axis displays the −log of p value (left). The orange points represent the ratio between the number of genes in group 4 that belong to that specific pathway by the total number of genes annotated to that specific pathway. (E) A diagram of the canonical pathway entitled "role of RIG1-like receptors in antiviral innate immunity." Genes highlighted in pink belong to group 4. IPS-1 (MAVS) is a central node of the pathway, linking RIG-1/MDA5 receptors to IRF7.

See also Figure S1.

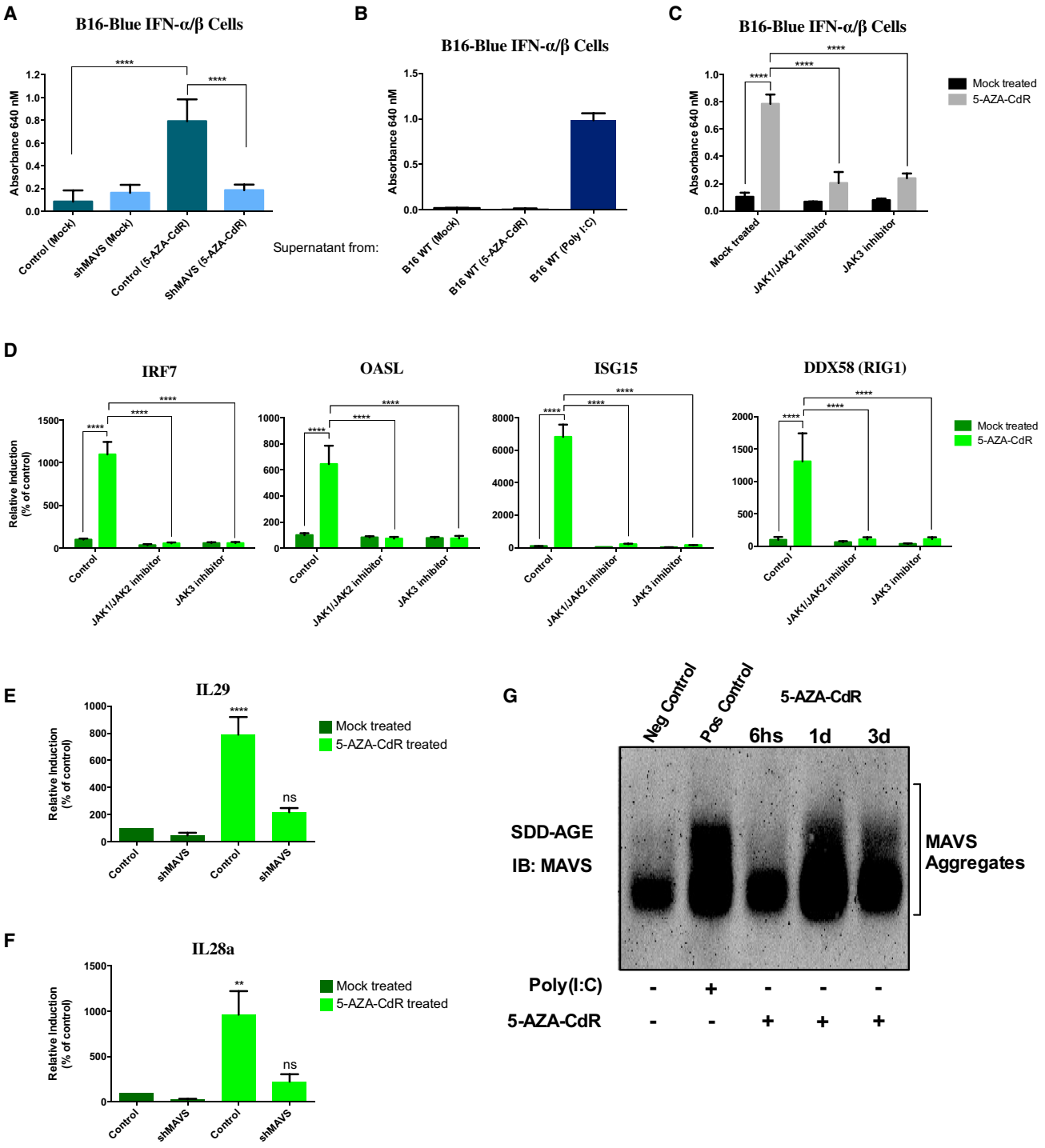

Figure 2. Transient Low-Dose Treatment of 5-AZA-CdR Induces Type III Interferon Production and Activation of MAVS

(A) B16-blue IFN-α/β cells (InvivoGen) were transiently treated with 0.3 μM of 5-AZA-CdR for 24 hr. Activity of the ISG54 promoter enhanced by a multimeric ISRE was determined by measuring secreted alkaline phosphatase (SEAP). SEAP activity was measured at 640 nm when the QUANTI-blue substrate was provided. The results presented are from three independent experiments. Error bars represent the SD of three independent experiments.

(B) Supernatants from B16 cells transiently treated with 5-AZA-CdR or transfected with 0.5 μg/ml of poly(I:C) were added to wild-type B16-blue IFN-α/β cells (InvivoGen), and the presence of bioactive IFNs-α/β was determined by measuring SEAP activity 24 hr after adding the supernatants. Error bars represent the SD of three independent experiments.

(C) B16-blue IFN-α/β cells (InvivoGen) were transiently treated with 5-AZA-CdR in the presence or absence of the JAK1/JAK2 inhibitor Ruxolitinib (1 μM) or the JAK3 inhibitor CP-690550 (1 μM). SEAP activity was measured at 640 nm.

(legend continued on next page)

with supernatant derived from wild-type (WT) B16 cells after 5-AZA-CdR treatment. The supernatant alone was not able to activate the SEAP reporter gene (Figure 2B), suggesting a lack of bioactive type I IFNs in the supernatant of wild-type B16 cells treated with 5-AZA-CdR. However, wild-type B16 cells transfected with poly(I:C) (positive control) were able to release type I IFNs in the supernatant, as shown by SEAP activation on B16-blue cells (Figure 2B). To test whether other cytokines could be playing a role in inducing the expression of interferon-responsive genes in response to 5-AZA-CdR, we treated the B16-blue cells with 5-AZA-CdR in the presence or absence of Ruxolitinib (JAK1/JAK2 inhibitor) or CP-690550 (JAK3 inhibitor). In the presence of either Ruxolitinib or CP-690550, 5-AZA-CdR treatment was no longer able to activate the SEAP reporter gene (Figure 2C). Since we could not detect type I IFNs and the B16-blue cells do not respond to IFN-γ, due to the inactivation of the IFN-γ receptor, these data suggest a potential role for type III IFNs.

Similarly to the B16 murine model, we observed that the co-treatment of 5-AZA-CdR with Ruxolitinib or CP-690550 was sufficient to block the ability of 5-AZA-CdR to induce the expression of four interferon-responsive genes (group 4) in the human colorectal cancer cell LIM1215 (Figure 2D), suggesting a potential role for type III IFNs. Indeed, we found that low-dose 5-AZA-CdR treatment was able to significantly increase the expression of the type III IFN IL29 in LIM1215, HCT116, and HT29 human colorectal cancer cell lines (Figures 2E and S2G–S2I). 5-AZA-CdR treatment also significantly increased the expression of the type III IFN IL28a in the LIM1215 cell line (Figures 2F and S2H–S2J). Altogether, our data suggest that transient low-dose 5-AZA-CdR treatment can induce the expression of type III, but not type I, IFNs, followed by a downstream activation of interferon-stimulated genes (ISGs) in a JAK-dependent manner.

Interestingly, when we knocked down MAVS (Figures S2C–S2F), we were able to repress the ability of 5-AZA-CdR treatment to induce type III IFNs (Figures 2E, 2F, and S2G–S2J), implicating an upstream role for the cytosolic pattern recognition receptors RIG1/MDA5 in initiating the signaling cascade induced by 5-AZA-Cd treatment that will culminate with type III IFNs and increase in expression of ISGs.

The ability of the mitochondrial protein MAVS to transduce the signal from the cytosolic pattern recognition receptors RIG1/MDA5 and activation of downstream IRFs to induce the expression of IFNs is dependent on the formation of very large prion-like aggregates of MAVS protein (Hou et al., 2011). To test whether the 5-AZA-CdR treatment is indeed inducing activation of RIG1/MDA5 and downstream signaling through MAVS, we isolated the mitochondrial fraction of LIM1215 treated with 5-AZA-CdR or poly(I:C) (positive control) (Figure S2K) and performed semi-denaturing detergent agarose gel electrophoresis (SDD-AGE), which has been previously shown to detect the formation of MAVS prion-like aggregates (Hou et al., 2011). We observed a smear of SDS-resistant high molecular weight MAVS aggregates in our positive control, as well as the treated cells, starting 1 day after 5-AZA-CdR treatment (Figure 2G), indicating a functional activation of MAVS.

Activation of Late-Response Genes Is Dependent on MDA5/MAVS/IRF7 Pathway Activation

Next, we sought to investigate the individual contributions of the cytosolic pattern recognition receptors RIG1 and MDA5. We knocked down RIG1 and MDA5 individually in LIM1215 cells using validated small hairpin RNAs (shRNAs) (Figure 3A). MDA5 knockdown was sufficient to inhibit the activation of group 4 genes after 5-AZA-CdR treatment, while RIG1 knockdown was able to partially reduce the activation of group 4 genes (Figure 3A). This result suggests a major role for MDA5 in mediating the downstream activation of MAVS after 5-AZA-CdR treatment. Indeed, when we knocked down MAVS (Figures S2C–S2F), we were also able to inhibit the activation of group 4 genes after 5-AZA-CdR treatment (Figures 3B, S3A, and S3B). It is important to note that knockdown of MAVS had no effect on the ability of 5-AZA-CdR to induce global DNA demethylation (Figures S5E–S5G).

MAVS activation is known to activate several downstream transcription factors, such as IRF1, IRF3, and IRF7 (Odendall et al., 2014; Seth et al., 2005). Next, we investigated which transcription factors are activated by MAVS in response to 5-AZA-CdR treatment. First, we performed IPA's upstream regulators analysis (Krämer et al., 2014) to identify transcription factors predicted to be activated based on the activation *Z* score of group 4 genes. We found IRF7 as one of the top predicted transcription factors, with 20 known IRF7 direct target genes also being upregulated in the group 4 gene set out of a total of 98 known IRF7 direct targets (p value of overlap: 5.09^{-15}; Figure 3C).

To validate that IRF7 was upregulated and activated, we performed confocal microscopy on the LIM1215 colorectal cancer cell line following 5-AZA-CdR treatment and observed increased protein levels of IRF7 and a robust nuclear translocation (Figure 3D, second row), indicating activation of this transcription factor. Moreover, in the presence of an impaired MDA5/MAVS pathway, by knockdown of MAVS, 5-AZA-CdR treatment is no longer sufficient to induce either IRF7 upregulation or activation, as measured by nuclear translocation (Figure 3D, fourth row). These data suggest that activation of interferon-responsive genes by 5-AZA-CdR treatment is mediated by MDA5/MAVS-dependent IRF7 activation, rather than by direct promoter DNA demethylation. Indeed, group 4 genes downstream of IRF7 have a significantly weaker anti-correlation between DNA

(D) The LIM1215 colorectal cancer cell line was transiently treated with 5-AZA-CdR in the presence or absence of the JAK1/JAK2 inhibitor Ruxolitinib (1 μM) or the JAK3 inhibitor CP-690550 (1 μM). Gene expression of four selected interferon-responsive genes was measured by quantitative real-time PCR at day 5.

(E and F) LIM1215 with or without shRNA against MAVS were transiently treated with 5-AZA-CdR. Gene expression of the type III interferon genes IL29 (E) and IL28a (F) was measured by quantitative real-time PCR at day 5.

(G) Mitochondrial extracts were prepared from LIM1215 cells treated with 5-AZA-CdR for the indicated time, or transfected with poly(I:C), and then aliquots of the extracts were analyzed by SDD-AGE. ****$p < 0.0001$; **$p < 0.01$ (one-way ANOVA).

See also Figure S2.

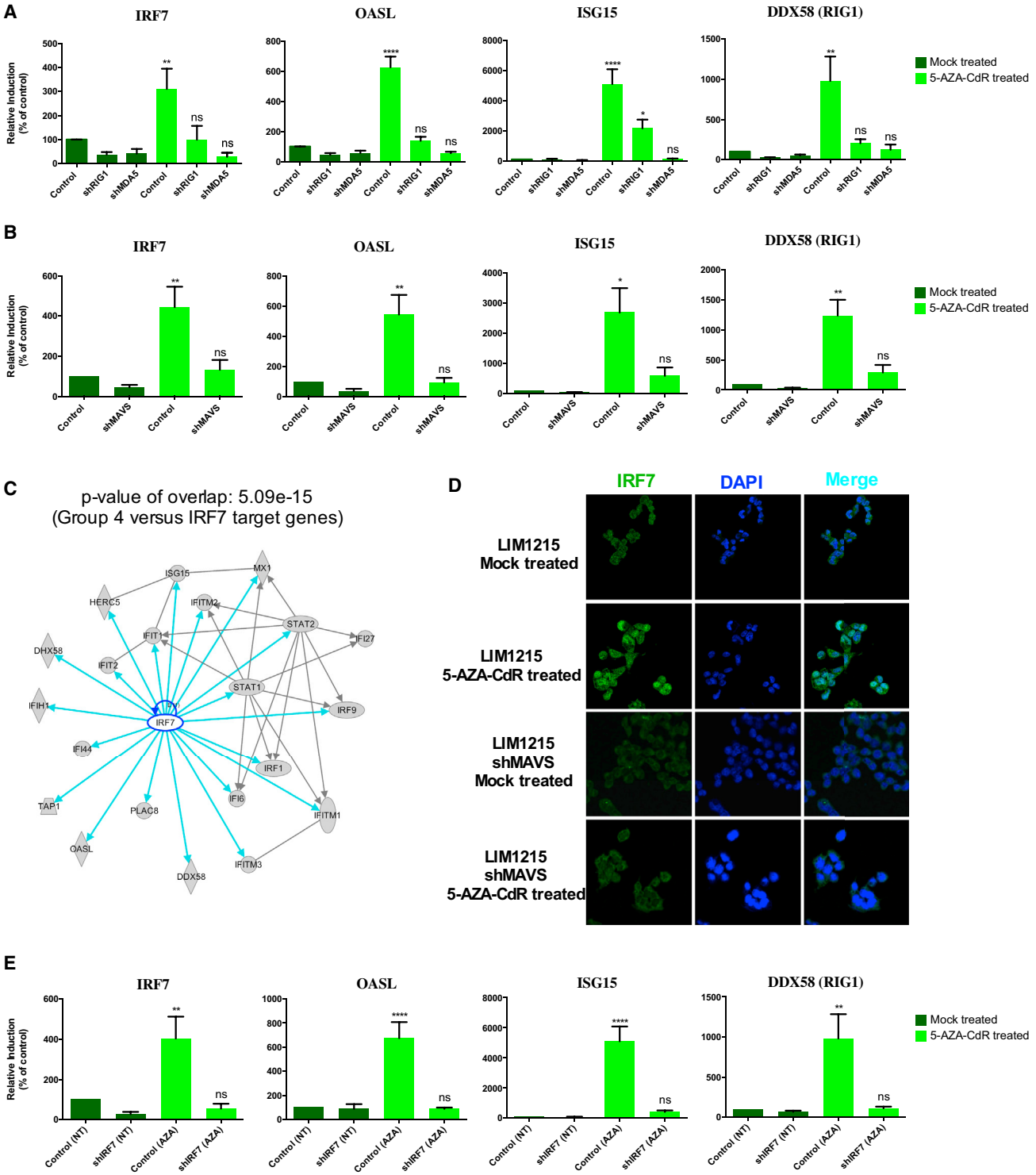

Figure 3. Activation of Interferon-Responsive Genes by a Transient Low-Dose Treatment of 5-AZA-CdR Is Dependent on MDA5/MAVS/IRF7 Activation

(A and B) The LIM1215 colorectal cancer cell line with or without shRNA against RIG1 (A), MDA5 (A), or MAVS (B) was transiently treated with 5-AZA-CdR. Gene expression of four selected interferon-responsive genes was measured by quantitative real-time PCR at day 5.

(C) Upstream regulators analysis using ingenuity pathway analysis reveals a significant overlap between group 4 genes and IRF7 direct target genes (p value: 5.09×10^{-15}).

(legend continued on next page)

methylation and gene expression than the rest of the group 4 genes (Figure S3C; Kolmogorov-Smirnov test of frequency distribution data; p value = 0.0004). Furthermore, we evaluated the DNA methylation levels of group 4 IRF7 downstream genes (Figure 3C) in a set of 125 colorectal cancer samples from different subgroups and 29 adjacent normal samples (Hinoue et al., 2012). Consistent with our previous data, these genes are largely unmethylated in primary samples, independent of the tumor/normal status and independent of the CIMP (CpG Island Methylator Phenotype) status (Figure S3D). Moreover, 5-AZA-CdR treatment did not induce IRF1 protein expression (Figure S3E), and it did not increase the levels of IRF3 (Figure S3F) or induce IRF3 nuclear translocation (Figure S3F), suggesting a major role for IRF7. To confirm the role of IRF7, we knocked down this transcription factor and observed that it was sufficient to inhibit the activation of group 4 genes after 5-AZA-CdR treatment (Figure 3E).

Altogether, our data suggest that transient low-dose 5-AZA-CdR treatment can induce activation of interferon-responsive genes by activating the MDA5/MAVS/IRF7 signaling pathway in a process independent of promoter DNA demethylation of interferon-responsive genes.

5-AZA-CdR Treatment Induces an Increase in dsRNAs

MDA5 is a cytosolic pattern-recognition receptor that recognizes dsRNAs associated with virus infections (Barbalat et al., 2011). Therefore, we investigated whether 5-AZA-CdR could be inducing a significant increase in dsRNAs, explaining the activation of the MDA5/MAVS/IRF7 pathway. Using the J2 antibody, a gold standard for dsRNA detection (Weber et al., 2006), confocal microscopy showed a significant increase in dsRNAs in LIM1215 cells starting 3 days after 5-AZA-CdR withdrawal (Figures 4A–4D), persisting for up to 10 days after drug withdrawal (Figures 4A–4D). Moreover, the second highest enriched pathway, identified in Figure 1D, has two components: "Regulation of innate immune response by RNA sensing molecules" and "Regulation of innate immune response by DNA sensing molecules." Remarkably, only the genes belonging to the RNA-sensing pathway were upregulated by transient low-dose 5-AZA-CdR treatment (Figures S4A and S4B).

It was recently reported that endogenous retrovirus (ERV) RNAs can trigger signaling by cytosolic pattern-recognition receptors and activate MAVS in mammals (Zeng et al., 2014). Therefore, we investigated whether ERVs could be the source of 5-AZA-CdR-induced dsRNA and the trigger for the antiviral response. Indeed, we observed a very robust and significant increase in transcription of human ERVs from classes previously described to trigger a MAVS-mediated response (Zeng et al., 2014) (Figure 4E). Then, using an RNase A protection assay under high-salt concentration (see the Experimental Procedures), we observed that ERVs transcripts were hundreds to thousands of times more resistant to RNase A digestion than a single-stranded RNA (ssRNA) gene (β-actin) in 5-AZA-CdR-treated cells (Figure 4F).

5-AZA-CdR Effects on Tumor Cell Growth Are Largely Dependent on the MDA5/MAVS/IRF7 Pathway

Transient low-dose 5-AZA-CdR treatment can decrease tumor cell growth and reduce colony formation (Kelly et al., 2010; Tsai et al., 2012; Yang et al., 2014). In order to test whether these anti-tumor effects are mediated by activation of the MDA5/MAVS/IRF7 pathway, we treated colorectal cancer cell lines with or without individual knockdowns of MDA5, MAVS, and IRF7. Population doubling time was monitored for up to 20 days, and we observed that the 5-AZA-CdR treatment exerted a durable increase in the population doubling time in all the three colorectal cancer cell lines as expected (Figures 5A–5C and S5A–S5C). However, knockdown of MDA5, MAVS, or IRF7 was sufficient to render these cells insensitive to 5-AZA-CdR treatment (Figures 5A–5C and S5A–S5C), even though the drug could still induce global DNA demethylation in the knockdown cells (Figures S5E–S5G). Important to note, MAVS knockdown alone has no major effect on population doubling time (Figure S5D). Interestingly, RIG1 knockdown was not sufficient to render these cells insensitive to drug treatment (Figure S5A), again suggesting a major role for MDA5 rather than for RIG1 in the response to 5-AZA-CdR treatment. These data suggest that the long-term effects on population doubling time are largely dependent on activation of the MDA5/MAVS/IRF7 pathway.

5-AZA-CdR Targets the Cancer-Initiating Compartment by Activation of the MDA5/MAVS/IRF7 Pathway

Next, we tested whether 5-AZA-CdR can target cancer-initiating cells (CICs), which are defined first and foremost by their ability to self-renew. To calculate the sphere-initiating frequency, we used the in vitro assay for sphere initiation followed by in vivo-limiting dilution assays (LDAs), the gold standard assay for measuring self-renewal (Kreso et al., 2014; Mack et al., 2014). For this assay, we plated 1, 10, 100, or 1,000 cells per well in a 96-well round-bottom plate for suspension cells, and after 4 weeks we counted the number of positive wells (i.e., with formation of a spheroid) (Figure 5D). Then we calculated the frequency of sphere-initiating cells using the previously described ELDA algorithm (Hu and Smyth, 2009). We used a pairwise chi-square test to calculate whether the frequencies of sphere-initiating cells were different between any two groups as previously described (Hu and Smyth, 2009; Kreso et al., 2014; Mack et al., 2014). Transient low-dose 5-AZA-CdR treatment induced a significant 10-fold reduction in the frequency of sphere-initiating cells (Figures 5E and 5F). However, inhibition of MDA5/MAVS/IRF7 activation by MAVS knockdown significantly reduced the ability of

(D) Confocal microscopy of LIM1215 cells after treatment with a transient low-dose of 5-AZA-CdR. Total IRF7 is stained in green, and nuclei are stained in blue (DAPI). There is increased IRF7 expression and nuclear translocation in 5-AZA-CdR-treated WT cells.

(E) LIM1215 colorectal cancer cell line with or without shRNA against IRF7 was transiently treated with 5-AZA-CdR. Gene expression of four selected interferon-responsive genes was measured by quantitative real-time PCR at day 5. The y axis represents the relative expression (in % of control) compared to the wild-type untreated control. Error bars represent the SD of at least three independent experiments. ns, non-significant; *p < 0.05; **p < 0.01; ****p < 0.0001 (one-way ANOVA).

See also Figure S3.

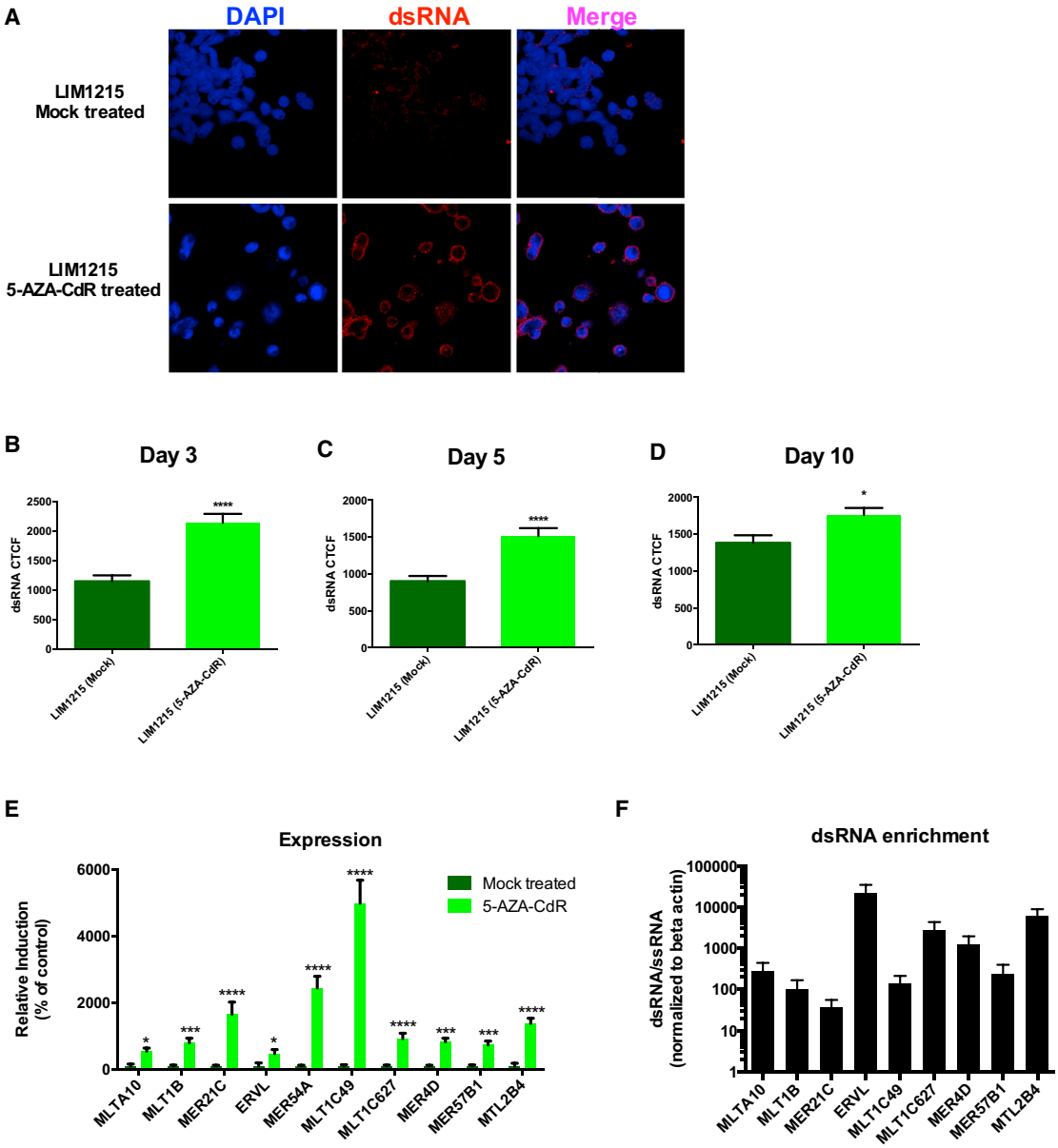

Figure 4. Increased dsRNA by a Transient Low-Dose Treatment of 5-AZA-CdR

(A) Confocal microscopy of LIM1215 cells 3 days after treatment with a transient low-dose of 5-AZA-CdR. Total dsRNA is stained in red, and nuclei are stained in blue (DAPI). There is increased dsRNA expression in the cytoplasm of 5-AZA-CdR-treated cells.

(B–D) Quantification of dsRNA performed by measuring cell fluorescence using ImageJ 3 days (B), 5 days (C) or 10 days (D) after 5-AZA-CdR treatment. Corrected total cell fluorescence (CTCF) was calculated using the following formula. CTCF = integrated density – (area of selected cell × mean fluorescence of background readings). ****$p < 0.0001$, *$p < 0.05$ (two-tailed t test).

(E) LIM1215 was transiently treated with 5-AZA-CdR. The expression level of ten selected ERVs was measured by quantitative real-time PCR at day 5. ****$p < 0.0001$; ***$p < 0.001$; *$p < 0.05$ (two-way ANOVA).

(F) Total RNA was extracted from 5-AZA-CdR-treated cells. RNA was then digested or not with 50 μg/ml RNase A in high-salt concentration (NaCl, 0.35 M) for 30 min. Enrichment of dsRNA over ssRNA was then calculated by normalizing the delta Ct between RNase A treated and non-treated of ERVs (dsRNA) against beta-actin (ssRNA). Error bars represent the SD of at least three independent experiments.

See also Figure S4.

5-AZA-CdR to target sphere-initiating cells (Figures 5E and 5F; p value = 0.000609), thereby suggesting that the effect of 5-AZA-CdR on self-renewal in the CIC fraction was dependent on MDA5/MAVS/IRF7 activation. Indeed, MDA5, but not RIG1, knockdown completely inhibited the ability of 5-AZA-CdR to target sphere-initiating cells (Figures S5H–S5J).

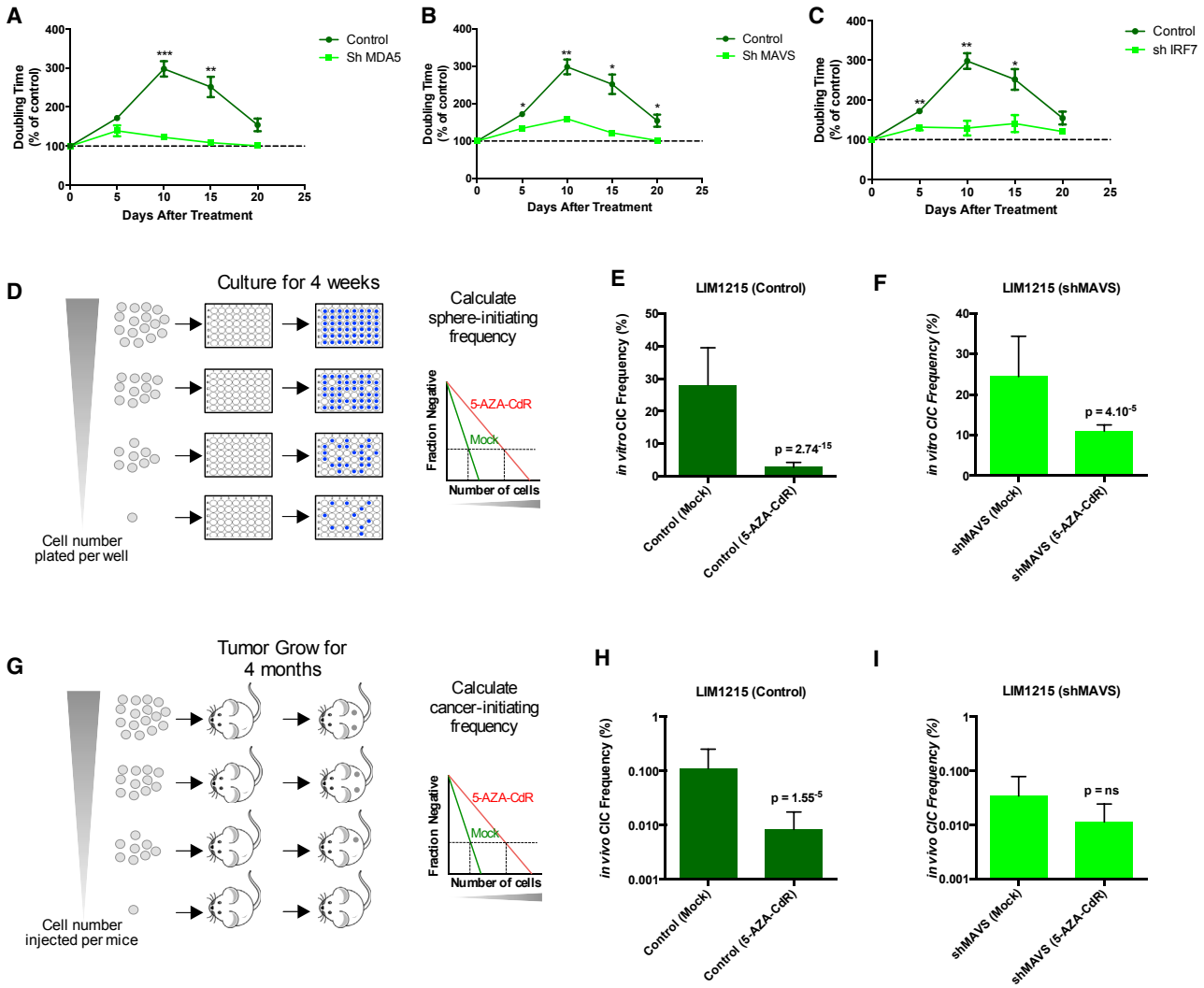

Figure 5. 5-AZA-CdR Effect on Cell Growth and Self-Renew Is Dependent on MDA5/MAVS/IRF7 Activation

(A–C) Population doubling time of LIM1215 with or without MDA5 (A), MAVS (B), and IRF7 (C) knockdown. The y axis denotes population doubling time (in hr) as a percentage of the vehicle-treated WT controls. The x axis represents time (in days) after 5-AZA-CdR withdrawal. Error bars represent the SD of three independent experiments.

(D) Schematic representation of the approach used to measure the sphere-initiating frequency after a transient low-dose 5-AZA-CdR treatment (see the Experimental Procedures).

(E and F) Frequency of LIM1215 CICs before and after a low-dose transient 5-AZA-CdR treatment measured by in vitro limiting dilution assay in wild-type (E) or shMAVS (F) cells. The y axis denotes the confidence intervals (lower, estimate and upper) for CIC frequency.

(G) Schematic representation of the approach used to measure the cancer-initiating cells frequency in vivo after a transient low-dose 5-AZA-CdR treatment (see the Experimental Procedures).

(H and I) Frequency of LIM1215 CICs before and after a low-dose transient 5-AZA-CdR treatment measured by in vivo limiting dilution assay in wild-type (H) or shMAVS (I) cells. The y axis denotes the confidence intervals (lower, estimate and upper) for CIC frequency. *$p < 0.05$; **$p < 0.01$; ***$p < 0.001$. Multiple t tests were used to test for difference in population doubling time. A pairwise chi-square test was used to test for the difference in CIC frequency.

See also Figure S5.

To validate our in vitro sphere-initiating results, we measured self-renewal using an in vivo-limiting dilution assay. NSG mice were injected subcutaneously with 10, 100, 1,000, 10,000, and 50,000 cells following a transient in vitro exposure to a low dose of 5-AZA-CdR or vehicle control. The presence or absence of tumors was assessed after 4 months so that the frequency of colorectal CICs could be calculated (Figure 5G). We observed that a transient low dose of 5-AZA-CdR significantly reduced colorectal CIC frequency in vivo (Figure 5H; p value = 0.0000155). However, blockage of MDA5/MAVS/IRF7 activation by MAVS knockdown rendered colorectal CICs completely insensitive to 5-AZA-CdR (Figure 5I).

We further investigated the potential of 5-AZA-CdR-mediated activation of MDA5/MAVS/IRF7 to target colorectal CICs using

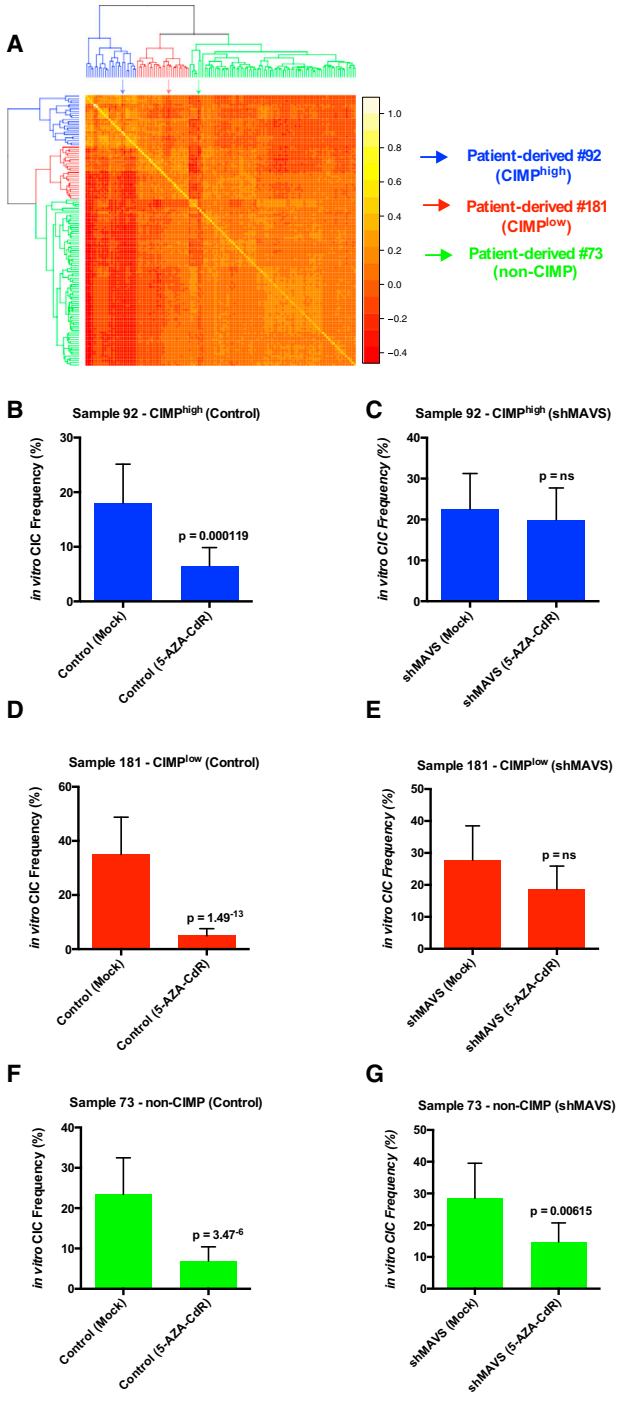

Figure 6. Transient 5-AZA-CdR Treatment Reduces the Frequency of Primary Colorectal CICs Independent of CIMP Status, and This Activity Is Dependent on MAVS Activation

(A) Colorectal patient-derived cells were classified according to their CpG Island Methylator Phenotype (CIMP) into CIMP^{high} (sample 92), CIMP^{low} (sample 181), and non-CIMP (sample 73). Primary tissue DNA methylation data and CIMP classifications were obtained from Hinoue et al. (2012). A heatmap shows the pairwise correlation using Spearman correlation method of each sample.

(B–G) The frequency of colorectal CICs before and after a low-dose transient 5-AZA-CdR treatment measured by an in vitro-limiting dilution assay in MAVS wild-type cells (B, D, and F) and in MAVS knocked-down (shMAVS) cells (C, E, and G). Patient-derived cells obtained from CIMP^{high} (sample 92) (B and C), a CIMP^{low} (sample 181) (D and E), and non-CIMP (sample 73) (F and G) were used. The y axis denotes the confidence intervals (lower, estimate and upper) for CIC frequency. A pairwise chi-square test was used to test for the difference in CIC frequency.

See also Figure S6.

primary colorectal cancer cells isolated at the time of surgical resection and stored in our biobank. Colorectal cancer samples can be divided into three major molecular subgroups based on the CpG Island Methylator Phenotype: CIMP^{high}, CIMP^{low}, or non-CIMP (Hinoue et al., 2012). By matching the global DNA methylation profile of our primary samples against publicly available DNA methylation data from primary colorectal cancer samples (Hinoue et al., 2012), we were able to classify our samples into the three DNA methylation subgroups (CIMP^{high}, CIMP^{low}, and non-CIMP; Figure 6A). Primary colorectal cancer cells were grown in a defined medium without serum, allowing for enrichment of CICs as previously described (Kreso et al., 2014; O'Brien et al., 2012). Using the same in vitro assay for sphere initiation coupled with LDAs (Figure 5D), we observed that 5-AZA-CdR treatment significantly reduced the frequency of sphere-initiating cells in the CIMP^{high} (Figure 6B), CIMP^{low} (Figure 6D), and non-CIMP (Figure 6F) cells. However, 5-AZA-CdR-mediated depletion of sphere-initiating cells was completely rescued when MAVS was knocked down in the CIMP^{high} (Figures 6C, S6A, and S6D) and CIMP^{low} (Figures 6E, S6B, and S6D) cells and partially rescued in the non-CIMP (Figures 6G, S6C, and S6D) cells. In agreement with our previous data, the ability of 5-AZA-CdR treatment to reduce the frequency of sphere-initiating cells in primary CRC samples was associated with a significant increase in dsRNA formation (Figures S6E–S6J).

Altogether, our data suggest that the majority of cell-intrinsic anti-tumor effects mediated by a transient low-dose 5-AZA-CdR treatment are mediated by activation of MDA5/MAVS/IRF7 pathway.

RIG1 and MDA5 Are Druggable Candidates for Targeting Colorectal CICs

Since low-dose 5-AZA-CdR treatment can target colorectal CICs by activation of the MDA5/MAVS/IRF7 pathway, we next investigated whether agonists to cytosolic pattern-recognition receptors alone are sufficient to reduce CIC frequency. Both RIG1 and MDA5 can recognize dsRNAs. RIG1 is preferentially activated by low molecular weight (LMW) dsRNAs, while MDA5 is preferentially activated by high molecular weight (HMW) dsRNAs (Kato et al., 2008). We transfected three primary colorectal cancer cells belonging to different CIMP status with LMW or HMW poly(I:C). Using the same in vitro assay for sphere initiation coupled with LDAs (Figure 5D), we observed that transfection of either LMW (RIG1 agonist) or HMW (MDA5 agonist) dsRNAs can significantly reduce the frequency of sphere-initiating cells in the CIMP^{high} (Figure 7A), CIMP^{low} (Figure 7B), and non-CIMP (Figure 7C) samples. However, agonists for other innate pattern-recognition receptors, such as cGAMP or flagellin, were unable to significantly reduce the frequency of

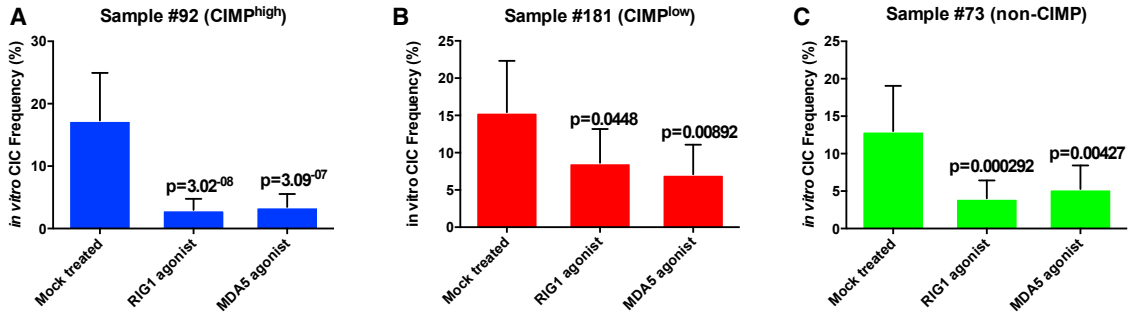

Figure 7. RIG1 or MDA5 Agonists Reduce the Frequency of Primary Colorectal CICs Independent of CIMP Status

(A–C) The frequency of colorectal CICs before and after transfection with 0.5 μg/ml of low molecular weight (LMW-RIG1 agonist) or high molecular weight (HMW-MDA5 agonist) poly(I:C) measured by an in vitro-limiting dilution assay. Patient-derived cells obtained from CIMP^{high} (sample 92) (A), CIMP^{low} (sample 181) (B), and non-CIMP (sample 73) (C) were used. The y axis denotes the confidence intervals (lower, estimate and upper) for CIC frequency. Pairwise chi-square test was used to test for the difference in CIC frequency.

See also Figure S7.

sphere-initiating cells in the CIMP^{high} (Figure S7A), CIMP^{low} (Figure S7B), and non-CIMP (Figure S7C) samples, corroborating our gene expression analysis, where we found enrichment only for regulation of innate immune response by RNA-sensing molecules (Figure S4).

These data suggest that the activation of RIG1 or MDA5 alone is sufficient to target colorectal CICs, highlighting the potential of these targets as druggable candidates to target colorectal CIC.

DISCUSSION

Recent clinical and experimental data have shown that low doses of 5-AZA-CdR induce sustained anti-tumor effects against solid cancers (Juergens et al., 2011; Tsai et al., 2012; Yang et al., 2014). However, the clinical response to low doses of DNA-demethylating agents in both solid tumors and MDS/AML usually takes more than a month to occur (Ahuja et al., 2014; Juergens et al., 2011; Treppendahl et al., 2014). This delayed response has led many people in the field to speculate that non-cytotoxic mechanisms may be playing a role in patient response. In addition, it has been suggested that this type of epigenetic therapy may be specifically targeting the cancer-initiating cell compartment (Ahuja et al., 2014; Tsai et al., 2012). However, it remains unclear whether transient low doses of 5-AZA-CdR could be targeting CICs and whether it is a direct consequence of its epigenetic effects.

Our data show that low doses of 5-AZA-CdR can significantly reduce the frequency of colorectal CICs using enriched sphere cultures derived from human colorectal cancer at the time of surgical resection. Colorectal cancer is a heterogeneous disease that can be classified into three main subgroups based on the DNA methylation profiles: CIMP^{high}, CIMP^{low}, or non-CIMP (Hinoue et al., 2012). Remarkably, we found that low doses of 5-AZA-CdR can strongly reduce the frequency of colorectal CICs independent of the CIMP profile, suggesting that this effect is elicited without demethylation of aberrantly methylated CpG islands.

Our data suggest that the durable anti-tumor effect of low-dose 5-AZA-CdR is actually mediated by induction of dsRNAs and activation of MDA5 RNA recognition receptor, followed by downstream activation of MAVS, IRF7, and type III IFNs and up-regulation of interferon-responsive genes, independent of their promoter demethylation. Moreover, clinical trials in non-small-cell lung cancer, breast cancer, and colorectal cancer patients with low-dose DNA-demethylating agents also identified up-regulation of interferon-responsive genes (Li et al., 2014; Wrangle et al., 2013), highlighting the clinical relevance of our results.

MDA5 is a pattern-recognition receptor (PRR) ubiquitously expressed in the cytoplasm of most human cells. MDA5 recognizes nucleic acids associated with viral infections (dsRNAs) and has two amino-terminal caspase recruitment domains (CARDs). The CARDs of MDA5, upon activation, can recruit the signaling adaptor protein MAVS (also known as IPS1, CARDIF, or VISA), which resides in the outer mitochondrial membrane. MAVS induces signaling cascades that result in nuclear translocation of IRF7 and activation of antiviral response programs, such as immunogenic cell death for viral clearance (Barbalat et al., 2011). Recent data suggest that the activation of RIG1 and MDA5 in tumor cells can also induce immunogenic cell death in melanoma, AML, and pancreatic cancer models (Besch et al., 2009; Duewell et al., 2014; Jiang et al., 2011). Moreover, this anti-tumor effect of RIG1/MDA5 signaling seems to be independent of type I interferon (Besch et al., 2009), similar to our results with 5-AZA-CdR.

Our data suggest that the 5-AZA-CdR-mediated activation of MDA5/MAVS/IRF7 pathway is a result of dsRNA induction of endogenous retrovirus (ERVs). This is in line with previous analyses suggesting that 5-AZA-CdR treatment could potentially induce dsRNAs by RNA polymerase III-driven bidirectional transcription of repetitive elements (Leonova et al., 2013) and with previous results showing that 5-AZA-CdR treatment can induce the expression of interferon-responsive genes and endogenous retrovirus (Karpf et al., 1999, 2004). Therefore, low-dose 5-AZA-CdR treatment will "trick" cancer cells into behaving as virus-infected cells, inducing an MDA5/MAVS/IRF7-dependent "viral mimicry" state.

Altogether, our results showing that low-dose 5-AZA-CdR targets colorectal CICs may explain the delayed response time

observed in patients undergoing clinical trials. Moreover, our results showing that the activation of MDA5/MAVS/IRF7 pathway by dsRNAs is the main mechanism responsible for the anti-tumor effects of low-dose 5-AZA-CdR may explain the current absence of DNA methylation markers for patient response. Monitoring dsRNA formation or MDA5/MAVS/IRF7 pathway activation may thereby be a better predictor of patient response than monitoring DNA methylation of promoters or gene bodies. Furthermore, our results suggest that by targeting the colorectal CICs, low-dose 5-AZA-CdR treatment may improve patient response to debulking therapies, such as standard of care chemotherapy, known to spare the CICs (Wicha, 2014). Remarkably, our results identify RIG1 and MDA5 cytosolic pattern recognition receptors as druggable targets against colorectal CICs.

EXPERIMENTAL PROCEDURES

See the Supplemental Experimental Procedures for detailed experimental procedures.

Chemical Treatment and Doubling Time Measurement

For each experiment, cells were plated 24 hr prior treatment. At day 0, cells were treated or mock treated with 5-AZA-CdR (0.3 μM; Sigma Aldrich). Cells were washed 24 hr after treatment and replenished with fresh media (without drug). Where indicated, Ruxolitinib (JAK1/JAK2 inhibitor) or CP-690550 (JAK3 inhibitor) was added at a concentration of 1 μg/ml. At the subsequent time points, cells were harvested, re-suspended, and counted; a fraction of cells were re-plated for the subsequent point. Doubling time (in days) was estimated as follows:

$$\text{Doubling time} = A^{*}\text{LOG}(2)/(\text{LOG}(B)\text{-LOG}(C)),$$

where A is the number of days since the cells were plated, B is the total number of cells when the cells were harvested, and C is the number of cells plated.

Total RNA Isolation, dsRNA Enrichment, and Real-Time PCR

Total RNA was extracted using TRIzol reagent. Primers are listed in Table S1. For dsRNA enrichment, RNA were treated or not for 30 min with 50 μg/ml RNaseA in high-salt concentration (NaCl, 0.35 M) to prevent dsRNA degradation (Life Technology). After treatment, RNase A was removed by RNA purification with TRIzol reagent. The thermal cycling protocol was one cycle at 95°C for 10 min and then 40 cycles at 95°C for 15 s, 60°C for 1 min, followed by a melting curve analysis. For each transcript, the efficiency of the PCR reaction was determined by the slope of the standard curve generated from a serial dilution. Each transcript level was normalized by the acidic ribosomal phosphoprotein P0 (RPLP0) housekeeping gene. For dsRNA enrichment, expression was normalized by β-actin (ssRNA).

Semi-denaturing Detergent Agarose Gel Electrophoresis

Semi-denaturing detergent agarose gel electrophoresis (SDD-AGE) was performed as previously described (Halfmann and Lindquist, 2008). Briefly, mitochondria were isolated (Qproteome Mitochondria Isolation Kit, Quiagen) from LIM1215 cells, resuspended in mitochondria buffer, and diluted before loading on a 1.5% agarose gel with 4× sample buffer (2X TAE 20% glycerol 8% SDS, bromophenol blue). Electrophoresis was done at 4°C at a constant voltage of 100 V in running buffer (1XTBE and 0.1% SDS) for 1 hr. Proteins were then transferred into a nitrocellulose membrane, and MAVS protein was detected using anti-MAVS antibody (1/1,000; Abcam).

Limiting Dilution Assay

For in vitro LDAs, colorectal cancer cells were treated or not with 5-AZA-CdR for 1 day, or transfected with 0.5 μg/ml of poly(I:C) low and high molecular weight in LyoVec, (InvivoGen) or treated with flagellin 1 μg/ml or transfected 0.5 μg/ml of cGAMP in LyoVec (Invivogen) for 3 days were dissociated into single cells. Cells were then seeded in 96-well plates at the indicated cell doses (1, 10, 100, and 1,000 cells/well). Trypan Blue was used to exclude dead cells. For each cell dose, at least 18 wells were seeded with cells, and for the lower cell doses, at least 72 wells were plated. 4 weeks later, wells containing spheres were scored, and the number of positive wells was used to calculate the frequency of sphere-forming units using the Extreme Limiting Dilution Analysis (ELDA) software (http://bioinf.wehi.edu.au/software/elda/index.html), provided by the Walter and Eliza Hall Institute (Hu and Smyth, 2009). The patient-derived colorectal CICs (#92, #181, and #73) were cultured as previously described (Kreso et al., 2014). Human colorectal cancer tissue was obtained with patient consent, as approved by the Research Ethics Board at the University Health Network.

For in vivo LDAs, LIM1215 cells were treated with and without 5-AZA-CdR for 24 hours. Following, single cells suspension was obtained and diluted serially to the desired cell doses. Cells were injected subcutaneously into the flanks of NSG mice. The number of tumors formed out of the number of sites injected was scored to determine the frequency of colorectal CICs calculated using the ELDA software. Animal work was carried out in compliance with the ethical regulations approved by the Animal Care Committee, University Health Network, Toronto, Ontario, Canada.

Statistical Analysis

LDA statistical analyses were performed using a pairwise chi-square test within the ELDA software as previously described (Hu and Smyth, 2009).

Pathway enrichment analysis and upstream regulators statistical analysis were performed using Fisher's exact test right-tailed within the IPA software as previously described (Krämer et al., 2014).

The statistical analysis to compare the frequency distribution was performed using a Kolmogorov-Smirnov test of frequency distribution data using GraphPad prism software. All other statistical analyses were performed using the GraphPad prism software.

ACCESSION NUMBERS

The accession number for all genome-wide DNA methylation data used in this study is GEO: GSE62086.

SUPPLEMENTAL INFORMATION

Supplemental Information includes Supplemental Experimental Procedures, seven figures, and one table and can be found with this article online at http://dx.doi.org/10.1016/j.cell.2015.07.056.

AUTHOR CONTRIBUTIONS

D.R. and D.D.C conceived of the work. D.R., G.L., P.A.J., C.O., and D.D.C. designed the experiments. D.R., H.L.Y., Y.W., S.Y.S., H.H., and D.D.C. performed the experiments. R.S., A.D., T.J.P., and D.D.C. analyzed the data. D.R. and D.D.C wrote the paper.

ACKNOWLEDGMENTS

Work in D.D.C.'s laboratory is supported by grants from the Cancer Research Society (CRS19092 and CRS19091), Canadian Cancer Society (CCSRI 703279 and CCSRI 703716), NSERC (489073), Ontario Institute for Cancer Research (OICR) with funds from the province of Ontario, the Princess Margaret Cancer Foundation, and the University of Toronto McLaughlin Centre (MC-2015-02). T.J.P. is supported by the Princess Margaret Cancer Foundation. P.A.J. is supported by grants from NCI (5R01CA082422) and Stand Up to Cancer.

Received: December 19, 2014
Revised: May 4, 2015
Accepted: June 26, 2015
Published: August 27, 2015

REFERENCES

Ahuja, N., Easwaran, H., and Baylin, S.B. (2014). Harnessing the potential of epigenetic therapy to target solid tumors. J. Clin. Invest. *124*, 56–63.

Barbalat, R., Ewald, S.E., Mouchess, M.L., and Barton, G.M. (2011). Nucleic acid recognition by the innate immune system. Annu. Rev. Immunol. *29*, 185–214.

Besch, R., Poeck, H., Hohenauer, T., Senft, D., Häcker, G., Berking, C., Hornung, V., Endres, S., Ruzicka, T., Rothenfusser, S., and Hartmann, G. (2009). Proapoptotic signaling induced by RIG-I and MDA-5 results in type I interferon-independent apoptosis in human melanoma cells. J. Clin. Invest. *119*, 2399–2411.

Dalerba, P., Dylla, S.J., Park, I.K., Liu, R., Wang, X., Cho, R.W., Hoey, T., Gurney, A., Huang, E.H., Simeone, D.M., et al. (2007). Phenotypic characterization of human colorectal cancer stem cells. Proc. Natl. Acad. Sci. USA *104*, 10158–10163.

De Carvalho, D.D., Sharma, S., You, J.S., Su, S.F., Taberlay, P.C., Kelly, T.K., Yang, X., Liang, G., and Jones, P.A. (2012). DNA methylation screening identifies driver epigenetic events of cancer cell survival. Cancer Cell *21*, 655–667.

Duewell, P., Steger, A., Lohr, H., Bourhis, H., Hoelz, H., Kirchleitner, S.V., Stieg, M.R., Grassmann, S., Kobold, S., Siveke, J.T., et al. (2014). RIG-I-like helicases induce immunogenic cell death of pancreatic cancer cells and sensitize tumors toward killing by CD8 T cells. Cell Death Differ. *21*, 1825–1837.

Halfmann, R., and Lindquist, S. (2008). Screening for amyloid aggregation by semi-denaturing detergent-agarose gel electrophoresis. J. Vis. Exp. *17*, 838.

Hinoue, T., Weisenberger, D.J., Lange, C.P., Shen, H., Byun, H.M., Van Den Berg, D., Malik, S., Pan, F., Noushmehr, H., van Dijk, C.M., et al. (2012). Genome-scale analysis of aberrant DNA methylation in colorectal cancer. Genome Res. *22*, 271–282.

Hou, F., Sun, L., Zheng, H., Skaug, B., Jiang, Q.X., and Chen, Z.J. (2011). MAVS forms functional prion-like aggregates to activate and propagate antiviral innate immune response. Cell *146*, 448–461.

Hu, Y., and Smyth, G.K. (2009). ELDA: extreme limiting dilution analysis for comparing depleted and enriched populations in stem cell and other assays. J. Immunol. Methods *347*, 70–78.

Issa, J.P., and Kantarjian, H.M. (2009). Targeting DNA methylation. Clin. Cancer Res. *15*, 3938–3946.

Jiang, L.J., Zhang, N.N., Ding, F., Li, X.Y., Chen, L., Zhang, H.X., Zhang, W., Chen, S.J., Wang, Z.G., Li, J.M., et al. (2011). RA-inducible gene-I induction augments STAT1 activation to inhibit leukemia cell proliferation. Proc. Natl. Acad. Sci. USA *108*, 1897–1902.

Juergens, R.A., Wrangle, J., Vendetti, F.P., Murphy, S.C., Zhao, M., Coleman, B., Sebree, R., Rodgers, K., Hooker, C.M., Franco, N., et al. (2011). Combination epigenetic therapy has efficacy in patients with refractory advanced non-small cell lung cancer. Cancer Discov. *1*, 598–607.

Karpf, A.R., Peterson, P.W., Rawlins, J.T., Dalley, B.K., Yang, Q., Albertsen, H., and Jones, D.A. (1999). Inhibition of DNA methyltransferase stimulates the expression of signal transducer and activator of transcription 1, 2, and 3 genes in colon tumor cells. Proc. Natl. Acad. Sci. USA *96*, 14007–14012.

Karpf, A.R., Lasek, A.W., Ririe, T.O., Hanks, A.N., Grossman, D., and Jones, D.A. (2004). Limited gene activation in tumor and normal epithelial cells treated with the DNA methyltransferase inhibitor 5-aza-2′-deoxycytidine. Mol. Pharmacol. *65*, 18–27.

Kato, H., Takeuchi, O., Mikamo-Satoh, E., Hirai, R., Kawai, T., Matsushita, K., Hiiragi, A., Dermody, T.S., Fujita, T., and Akira, S. (2008). Length-dependent recognition of double-stranded ribonucleic acids by retinoic acid-inducible gene-I and melanoma differentiation-associated gene 5. J. Exp. Med. *205*, 1601–1610.

Kelly, T.K., De Carvalho, D.D., and Jones, P.A. (2010). Epigenetic modifications as therapeutic targets. Nat. Biotechnol. *28*, 1069–1078.

Krämer, A., Green, J., Pollard, J., Jr., and Tugendreich, S. (2014). Causal analysis approaches in Ingenuity Pathway Analysis. Bioinformatics *30*, 523–530.

Kreso, A., and Dick, J.E. (2014). Evolution of the cancer stem cell model. Cell Stem Cell *14*, 275–291.

Kreso, A., van Galen, P., Pedley, N.M., Lima-Fernandes, E., Frelin, C., Davis, T., Cao, L., Baiazitov, R., Du, W., Sydorenko, N., et al. (2014). Self-renewal as a therapeutic target in human colorectal cancer. Nat. Med. *20*, 29–36.

Leonova, K.I., Brodsky, L., Lipchick, B., Pal, M., Novototskaya, L., Chenchik, A.A., Sen, G.C., Komarova, E.A., and Gudkov, A.V. (2013). p53 cooperates with DNA methylation and a suicidal interferon response to maintain epigenetic silencing of repeats and noncoding RNAs. Proc. Natl. Acad. Sci. USA *110*, E89–E98.

Li, H., Chiappinelli, K.B., Guzzetta, A.A., Easwaran, H., Yen, R.W., Vatapalli, R., Topper, M.J., Luo, J., Connolly, R.M., Azad, N.S., et al. (2014). Immune regulation by low doses of the DNA methyltransferase inhibitor 5-azacitidine in common human epithelial cancers. Oncotarget *5*, 587–598.

Mack, S.C., Witt, H., Piro, R.M., Gu, L., Zuyderduyn, S., Stütz, A.M., Wang, X., Gallo, M., Garzia, L., Zayne, K., et al. (2014). Epigenomic alterations define lethal CIMP-positive ependymomas of infancy. Nature *506*, 445–450.

Merlos-Suárez, A., Barriga, F.M., Jung, P., Iglesias, M., Céspedes, M.V., Rossell, D., Sevillano, M., Hernando-Momblona, X., da Silva-Diz, V., Muñoz, P., et al. (2011). The intestinal stem cell signature identifies colorectal cancer stem cells and predicts disease relapse. Cell Stem Cell *8*, 511–524.

Navada, S.C., Steinmann, J., Lübbert, M., and Silverman, L.R. (2014). Clinical development of demethylating agents in hematology. J. Clin. Invest. *124*, 40–46.

O'Brien, C.A., Pollett, A., Gallinger, S., and Dick, J.E. (2007). A human colon cancer cell capable of initiating tumour growth in immunodeficient mice. Nature *445*, 106–110.

O'Brien, C.A., Kreso, A., Ryan, P., Hermans, K.G., Gibson, L., Wang, Y., Tsatsanis, A., Gallinger, S., and Dick, J.E. (2012). ID1 and ID3 regulate the self-renewal capacity of human colon cancer-initiating cells through p21. Cancer Cell *21*, 777–792.

Odendall, C., Dixit, E., Stavru, F., Bierne, H., Franz, K.M., Durbin, A.F., Boulant, S., Gehrke, L., Cossart, P., and Kagan, J.C. (2014). Diverse intracellular pathogens activate type III interferon expression from peroxisomes. Nat. Immunol. *15*, 717–726.

Ricci-Vitiani, L., Lombardi, D.G., Pilozzi, E., Biffoni, M., Todaro, M., Peschle, C., and De Maria, R. (2007). Identification and expansion of human colon-cancer-initiating cells. Nature *445*, 111–115.

Seth, R.B., Sun, L., Ea, C.K., and Chen, Z.J. (2005). Identification and characterization of MAVS, a mitochondrial antiviral signaling protein that activates NF-kappaB and IRF 3. Cell *122*, 669–682.

Treppendahl, M.B., Kristensen, L.S., and Grønbæk, K. (2014). Predicting response to epigenetic therapy. J. Clin. Invest. *124*, 47–55.

Tsai, H.C., Li, H., Van Neste, L., Cai, Y., Robert, C., Rassool, F.V., Shin, J.J., Harbom, K.M., Beaty, R., Pappou, E., et al. (2012). Transient low doses of DNA-demethylating agents exert durable antitumor effects on hematological and epithelial tumor cells. Cancer Cell *21*, 430–446.

Weber, F., Wagner, V., Rasmussen, S.B., Hartmann, R., and Paludan, S.R. (2006). Double-stranded RNA is produced by positive-strand RNA viruses and DNA viruses but not in detectable amounts by negative-strand RNA viruses. J. Virol. *80*, 5059–5064.

Wicha, M.S. (2014). Targeting self-renewal, an Achilles' heel of cancer stem cells. Nat. Med. *20*, 14–15.

Wrangle, J., Wang, W., Koch, A., Easwaran, H., Mohammad, H.P., Vendetti, F., Vancriekinge, W., Demeyer, T., Du, Z., Parsana, P., et al. (2013). Alterations of immune response of Non-Small Cell Lung Cancer with Azacytidine. Oncotarget *4*, 2067–2079.

Yang, X., Han, H., De Carvalho, D.D., Lay, F.D., Jones, P.A., and Liang, G. (2014). Gene body methylation can alter gene expression and is a therapeutic target in cancer. Cancer Cell *26*, 577–590.

Zeng, M., Hu, Z., Shi, X., Li, X., Zhan, X., Li, X.D., Wang, J., Choi, J.H., Wang, K.W., Purrington, T., et al. (2014). MAVS, cGAS, and endogenous retroviruses in T-independent B cell responses. Science *346*, 1486–1492.